Enhanced Chiral Exciton Coupling

in Neat Molecular Films

Yoichi Sasaki,[†,§] Jérôme Gautier,[†,#] Minghao Li,[†,¶] Lydia Karmazin,[‡] Thomas W. Ebbesen,[†,*] Cyriaque Genet[†,*]

† University of Strasbourg and CNRS, CESQ & ISIS (UMR 7006) and icFRC, 8 allée G. Monge, 67000 Strasbourg, France

‡ University of Strasbourg and CNRS, Institut de Chimie (UMR 7177), 1 rue B. Pascal, 67000 Strasbourg, France

AUTHOR INFORMATION

Corresponding Author

*ebbesen@unistra.fr

*genet@unistra.fr

ABSTRACT.

Chiral molecule-based organic thin films are of increasing interest in optoelectronics and light technologies where the development of isotropic neat films of chiral molecules is important for practical applications. Understanding the chiroptical responses of dense molecular aggregates often becomes challenging due to the reflection or scattering of light arising from significant reflectivity changes at the excitonic transition. Furthermore, the combination of linear birefringence (LB) and linear dichroism (LD) from micro- to mesoscopic ordering is a potential source of artifacts. Here we report the circular dichroism (CD) of optically isotropic neat films of a new BODIPY−BINOL conjugate (*O*-BODIPY) which reveals a negligible LD-LB contribution as measured with both conventional methods and Mueller polarimetry. A 5-fold increase in the anisotropy factor in the neat film relative to the solution is explained by intermolecular exciton coupling. Time-dependent density functional theory calculations of possible intermolecular geometries induced in the film indicate the formation of short-ordered structures in the isotropic film with the help of combined chiral units. These results provide insight into chiral light−matter interactions, which are currently at the core of many fundamental discussions and promising chiroptical applications.

KEYWORDS Chiral molecule, Circular dichroism, Exciton coupling, Mueller polarimetry

Chiral light−matter interactions that exploit the spin angular momentum of light in relation to specific electronic transitions of matter have attracted much attention for potential applications, such as biosensing,[1−4] chemical synthesis,[5,6] and the development of new optical devices.[7−10] The strength of the light−matter interactions is determined by the real and imaginary parts of the refractive index of the materials. In regard to chiroptical signatures, chiral features can be controlled by the molecular structure and the macroscopic ordering. Recent advances in synthesizing chiral molecular systems ranging from small molecules to large supramolecular assemblies provide new strategies to put to work the intimate relationship between such molecular structures and chiroptical responses, paving the way for handedness selective manipulation of light.[10]

Circular dichroism (CD) is a standard chiroptical property of molecular-based chiral materials, with an associated spectrum that is dependent on molecular structures and intermolecular interactions. Since CD depends on absorption, i.e., optical path length, the absorption dissymmetry factor g_{abs} (where $g_{abs} \equiv 2(A_L - A_R)/(A_L + A_R)$) is also used to evaluate the intrinsic chiroptical response. Typical CD values for usual molecules are weak, resulting in g_{abs} values in the range of 10^{-4} to 10^{-3},[11,12] where A_L and A_R denote the respective absorption of left- and right-handed light, respectively, through the chiral material. The CD value is related to the rotational strength R_{eg}[11]

$$R_{eg} = Im(\langle g|\hat{\mu}|e\rangle \cdot \langle e|\hat{m}|g\rangle) \quad (1)$$

that involves the imaginary part of the scalar product of the electric and magnetic dipoles induced by light, where $\hat{\mu}$ and $\hat{m}$ refer to the magnetic and electric dipole operators, respectively, taken between the ground (g) and excited (e) states. To get a nonvanishing R_{eg}, a simple strategy is to combine a π-conjugated system with a chiral moiety,[13−19] which produces a magnetic dipole moment along the same direction as the electric one.

Recently, Sánchez-Carnerero et al. demonstrated that a conjugate of an achiral BODIPY with a chiral BINOL (*O*-BODIPY) shows both CD and circularly polarized light emission in the visible range above wavelengths of 500 nm.[14] Thanks to the simplicity of the synthesis, a new variety of *O*-BODIPY compounds has been developed that absorbs light from the ultraviolet to the near-infrared ranges of the optical spectrum.[20−25]

In condensed molecular aggregates, where more than two chromophores are close to each other, exciton coupling also contributes to nonvanishing R_{eg}. The CD derived from exciton coupling shows a bisignated spectrum.[26] Since the sign and intensity of the spectrum are correlated with the intermolecular geometries and dipolar interactions, a series of chiral molecular systems has been designed to search for optimal chiroptical responses.[11] Importantly, effective usage of exciton coupling has recently enabled reaching g_{abs} values larger than 10^{-2},[27] which are much larger than the typical values of isolated chiral molecules ($g_{abs} < 10^{-3}$). To further optimize such systems for practical applications, it is essential to understand the relationship between the

molecular structure and the optical response, including the electronic structure in aggregated phases.[28]

Strong chiral light−matter interactions in organic neat films have the potential to allow for the manipulation of the polarization properties of light at the nanoscale. However, the nature of the film requires the careful assessment of its polarimetric properties with respect to potential artifacts.[29−32] Microscopic to mesoscopic ordering of dense molecular aggregates indeed results in optical anisotropic features such as linear birefringence (LB) and linear dichroism (LD) that can contaminate circular dichroism (CD) and birefringence (CB) signals, as observed already in polymer films.[31,33] In addition, reflection and scattering at the film−air interface lead to an overestimation of the absorption and to a potential limitation of depolarization effects, respectively. To fully characterize samples including depolarization, Mueller matrix polarimetry has been introduced as the right methodology.[34−37] Thickness-dependent absorbance (−log(T)) measurements combined with Mueller polarimetry have been performed to provide measurements of the g_{abs} of functionalized squaraine films that are intrinsic (thickness-independent).[35]

Here, we designed a new *O*-BODIPY derivative (*O*-BDPhR1/S1, Figure 1a) and investigated the optical response of neat films made of such a derivative with both conventional methods and Mueller polarimetry. With the help of the asymmetric chiral BINOL structure and the introduction of a phenyl ring, an optically isotropic thin film with a highly smooth surface was obtained (Figures 1b and S4) with negligible polarization artifacts, as described next. The outstanding optical qualities (see below) of the thin films yielded absorption dissymmetry factors that were 5 times larger than a solution of *O*-BDPhR1/S1 in toluene. This very large enhancement

of the chiroptical response points to specific molecular geometries in the isotropic neat film. Such geometries are discussed on the basis of the single-crystal structure of *O*-BDPhS1 and using time-dependent density functional theory (TD-DFT) calculations.

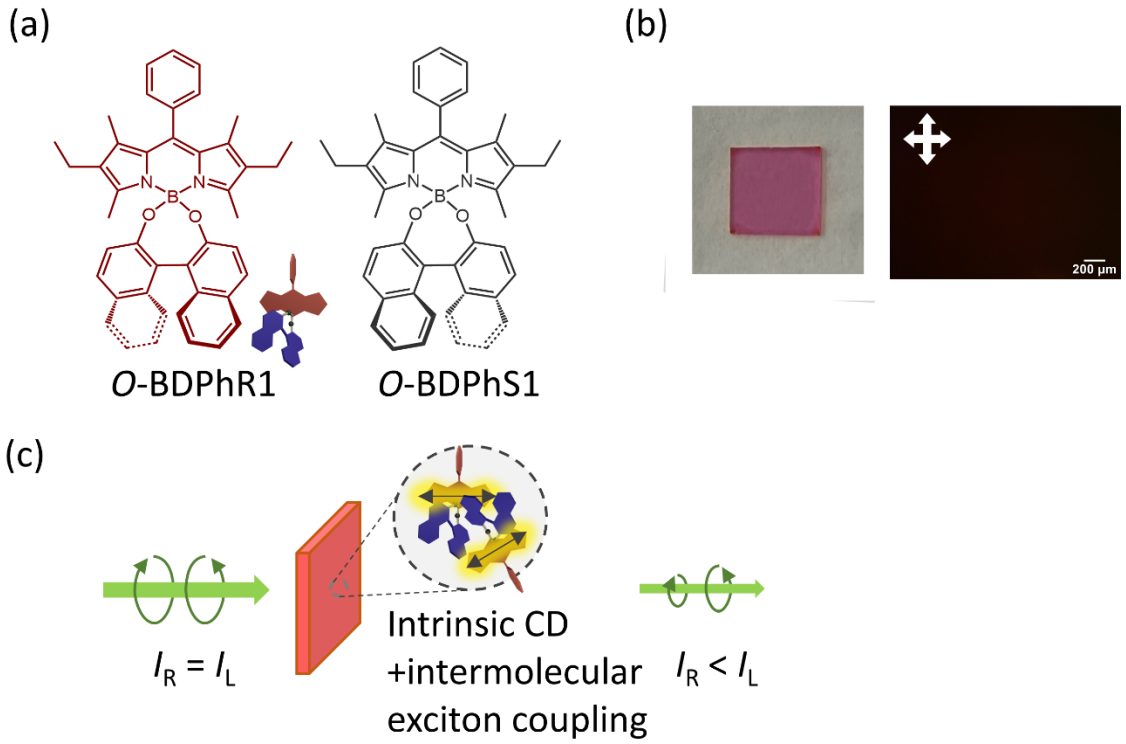

Figure 1. (a) Chemical structure of *O*-BDPhR1/S1. (b) Photographic image of a spin-coated film of *O*-BDPhS1 together with a reflection light microscopy image under crossed polarizers. (c) Graphical image of the neat film stressing the importance of the combination of both intrinsic CD and intermolecular exciton coupling in the transmission.

The basic photophysical properties of *O*-BDPhR1/S1 in toluene were consistent with the reported values for *O*-BODIPY (Figure 2).[30] The lowest transition of the BODIPY−BINOL at 528 nm has been assigned to the π−π* transition along the long axis of BODIPY.[38] The optical activity

measured at that transition is understood to be due the electronic dipole associated with the π–π* transition of BODIPY now coupled to the magnetic dipole associated with the BINOL chiral unit.[39] The absorption dissymmetry factor of *O*-BDPhR1/S1 was calculated to be 1.1×10^{-3}. We note that the introduction of the phenyl ring did not affect the electronic energy, most probably because the steric hindrance of hydrogens makes the phenyl ring orthogonal to the BODIPY backbone, which does not extend the π-conjugation.

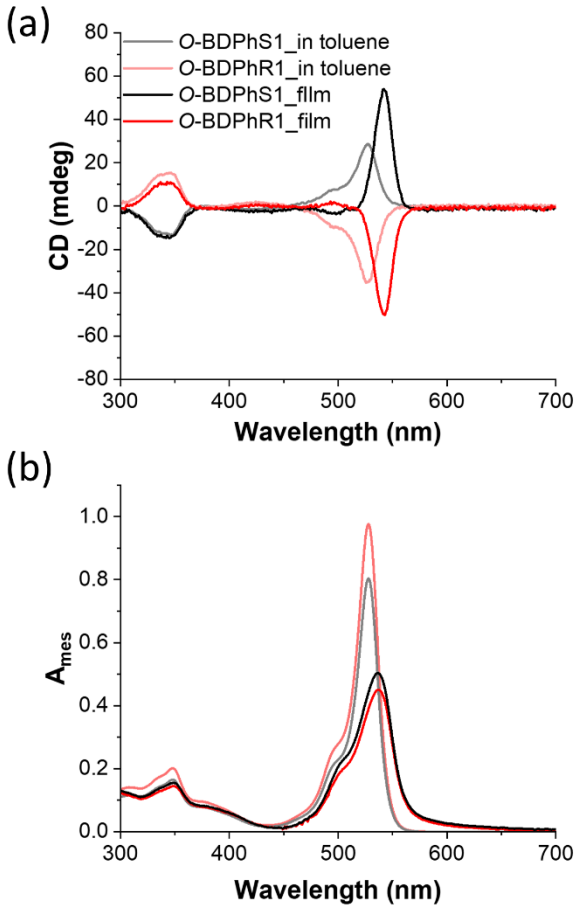

Figure 2. (a) CD and (b) absorbance spectra of *O*-BDPhR1/S1 both in toluene and in the neat film. These spectra have been obtained by using a conventional CD spectrometer where the LB and LD are not considered.

After spin coating the concentrated solution on a clean glass substrate, *O*-BDPhR1/S1 forms a transparent neat film with significantly enhanced CD intensity (Figures 1b and 2a). The isotropic feature of the film was confirmed by a crossed-polarized image (Figure 1b). AFM imaging showed that the root-mean-square (RMS) roughness of the film is very low (0.29 nm RMS, Figure S4), bringing light scattering at the surface to negligible levels in the visible range. This gave our system a clear optical advantage: the absolute absorption of the film can be evaluated by recording only the transmission and reflection spectra. The CD intensity at wavelengths around the lowest π−π* transition of the BODIPY unit at 528 nm was enhanced significantly, while the one around 340 nm attributed to the π−π* transition of the BINOL units[40] remained practically unchanged. The observed enhancement is due to exciton-coupled CD, which emerges when molecules are close to each other with fixed geometries in the condensed phase, indicating the limited number of relative intermolecular geometries available in the neat film without mesoscopic ordering. We stress that the expected bisignation typical of exciton-coupled CD was not observed (see a similar observation reported by Schultz et al. [35]), probably because the negative branch (at a lower energy) of the exciton-coupled CD is spectrally compensated for by the positive CD band associated with the monomeric species. The observed enhancement led us to study different aggregate geometries that can be made possible within the film based on the single-crystal analysis and the TD-DFT calculations, as reported below.

Single crystals of *O*-BDPhS1 were obtained through recrystallization. The compound crystallized in the chiral orthorhombic $P2_12_12_1$ space group (Figures S5 and S6, Table S1). In the crystal, there are pairs of *O*-BDPhS1 with a twisted and tilted geometry (geometry 1, Figures 3a and S6a) that from a one-dimensional *J*-type arrangement along the a-axis (geometry 2, Figures 3b and S6b). Investigating these geometries gives us clues about understanding the enhanced CD spectrum in the isotropic neat film. We also found that solvent vapor annealing for the neat film with toluene induces crystallization (Figure S7a). The X-ray diffraction (XRD) pattern of the annealed film was almost the same as the one from the crystalline powder with the $P2_12_12_1$ form (Figure S7d) only; no other polymorphs were observed.

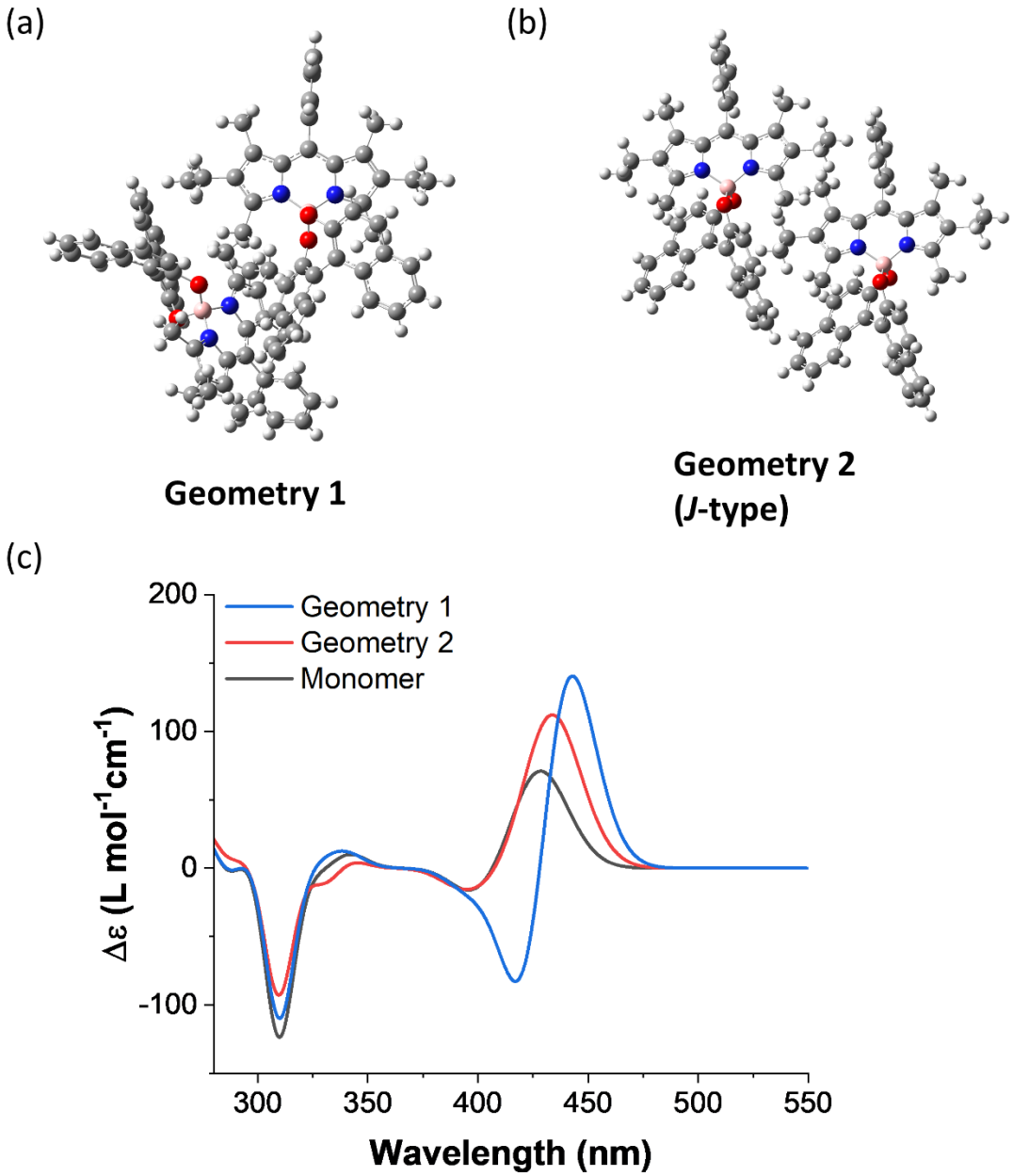

Figure 3. (a and b) Intermolecular geometries of dimers of *O*-BDPhS1 found in the crystal structure. (c) Calculated electronic CD spectra of *O*-BDPhS1 based on TD-DFT (6-31G(d)).

For the closest two geometries (1 and 2) extracted from the crystal structure, we conducted TD-DFT calculations to obtain the electronic CD spectra (Figure 3c). Geometry 1 gave a positive couplet around the lowest transition of *O*-BDPhS1 in energy. In contrast, for geometry 2, the CD signal was similar to the monomer results, as expected since the *J*-type geometry 2 has two parallel

dipoles. Although the energy levels do not exactly match with the experimental absorbance and CD spectra, the geometries satisfactorily explain the trends observed in the neat film. We also noted small red shifts on the absorbance spectra (Figure 2b) that reveal the presence of intermolecular dipole interactions. This led us to conclude that the total CD in Figure 2a can be explained by the combination of contributions coming from the monomeric CD and from the Frenkel-exciton-like coupled species in geometry 1. The negative signals of the exciton-coupled CD from geometry 1 that originated from the π−π* transitions of BODIPY could be partly compensated for by the CD from monomeric species. Other geometries with different relative orientations and distances are expected due to the isotropic feature, but their contributions are hardly detectable experimentally. Precise assignment of the two dips was difficult because of the accuracy of the current theoretical calculation results. Note that the DFT accuracy of the determination of the energy levels for *O*-BODIPY could be improved by a proper account of the vibrational structure.[39]

To unveil the relationship between the intermolecular distance and the exciton coupling of the *O*-BDPhR1/S1 film, concentration-dependent CD spectra were measured (Figure 4a). We mixed *O*-BDPhS1 with polystyrene and prepared films following the same methodology used for the neat films. As the concentration of *O*-BDPhS1 was increased, the peak of the CD showed a red shift accompanied by the emergence of small dips around 495 and 515 nm (Figure 4a) which most probably are the traces of the negative components of the exciton-coupled CD signals discussed above. Due to the significant change of the refractive index around the electronic absorption, correcting for the reflection that underestimated the absorption was necessary to obtain the right dissymmetry factor of the neat film ($g_{abs,exp}$, $g_{abs,cor}$, Figures 4b and S8). These results directly

point toward the role played by the interactions between the molecules in the measured enhancement values.

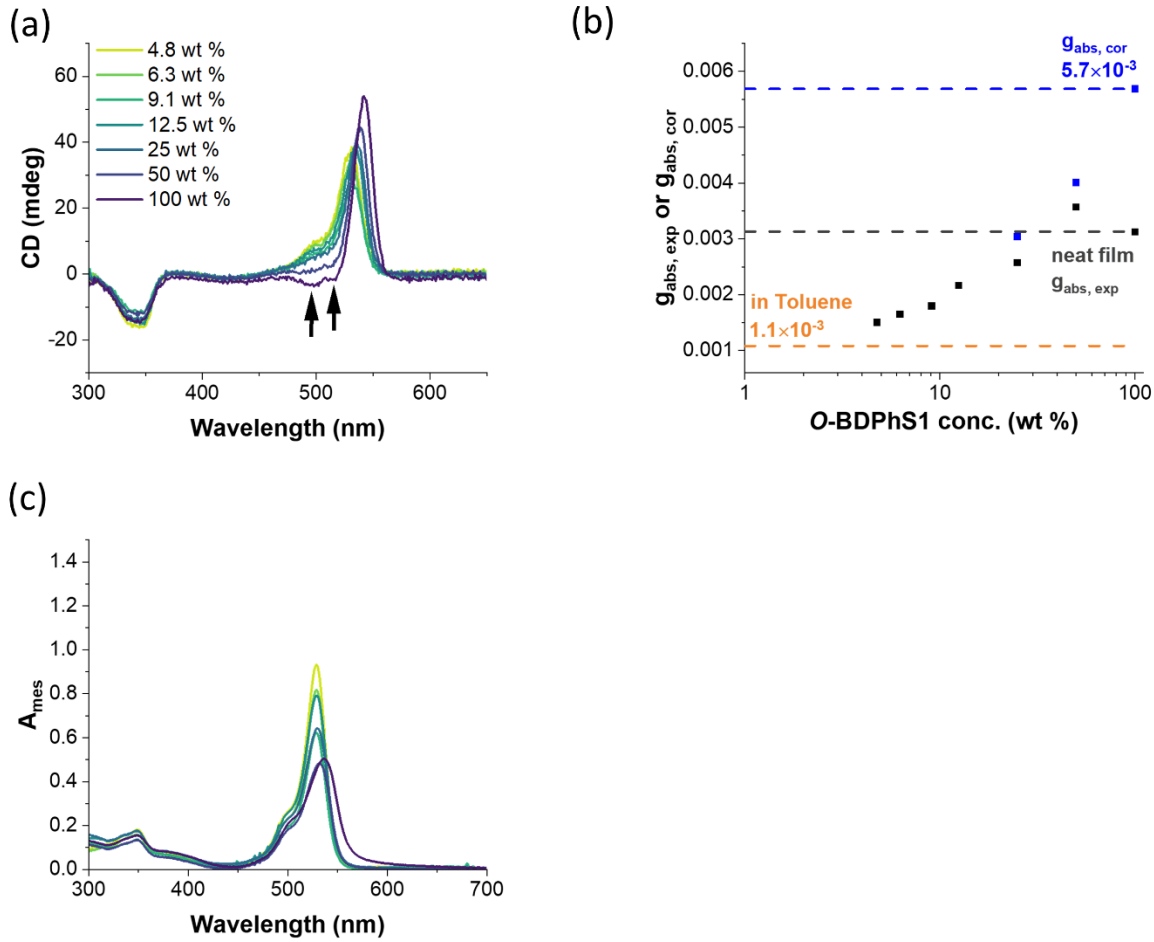

Figure 4. Concentration-dependent (a) CD, (b) $g_{abs,exp}$ and $g_{abs,cor}$, (c) and absorbance spectra of *O*-BDPhS1 in polystyrene ranging from at 4.8−100 wt %. The arrows in (a) point to the dips at ca. 495 and 515 nm that emerged at high concentrations. The dashed lines in (b) denote the g_{abs} of *O*-BDPhS1 in toluene (orange), the neat film (black), and the reflection-corrected g_{abs} of the neat film ($g_{abs,cor}$, blue). Note the conditions at 100 wt % correspond to the neat film limit.

As a control of the CD spectra, Mueller polarimetry was conducted for the neat films (Figures 5, S9, and S10). On such films, the LD and LB components could indeed potentially spoil a reliable CD measurement. It turned out that as measured, such LD-LB components were negligibly small, indicating that the CD signals are of intrinsic nature and not emerging from macroscopic sources of anisotropy. The CD spectra of both enantiomers showed a mirror image with the expected Kramers−Kronig relation between the CB and the CD. Thanks to the very smooth surfaces of our films, the second asset of our chiroptical molecular material, depolarization, was also negligible throughout the measured wavelength range (Figure S10). This outstanding optical quality of the film not only validates the reflection correction performed but also perfectly justifies the Mueller matrix differential decomposition method (see Experimental Methods).

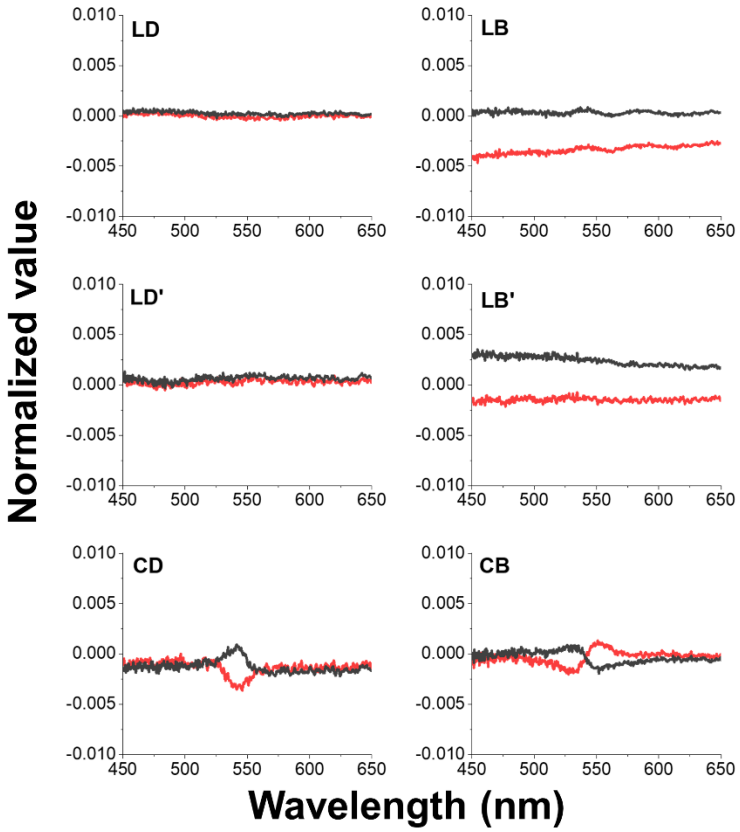

Figure 5. Chiroptical polarization quantities associated with neat films made of *O*-BDPhR1 (red) and *O*-BDPhS1 (gray) calculated after performing a differential decomposition of the Mueller matrices. Each matrix is recorded for each enantiopure neat film that we prepared.

In addition, the importance of the covalent conjugation for the enhancement was confirmed by a control experiment with a nonconjugated hybrid material of an achiral BODIPY (A1, Figure S11a) and a chiral BINOL derivative (C1, Figure S11a). The spin-coated film of A1−C1 (A1:C1 = 1:1) had negligible LD, LB, CD, and CB components (Figure S11c). The molecular distance between A1 and C1 in this case is expected to be large, which does not provide a chiral environment for A1. This proved that the achiral (BODIPY)−chiral (BINOL) conjugation is necessary to obtain the CD enhancement seen in the *O*-BDPhR1/S1 films.

To conclude, the chiral BINOL structure of *O*-BDPhR1/S1 results in intermolecular exciton coupling that enhances the absorption dissymmetry factor by a factor of 5 in the condensed phases. Thanks to the asymmetric structure of BINOL and the weak intermolecular interactions among the molecules, *O*-BDPhR1/S1 forms an isotropic neat film with a smooth surface, which gives negligible LD-LB signatures and very low levels of depolarization. These exceptionally good optical features are promising for exploring more complex chiroptical systems obtained, for instance, by coupling such *O*-BODIPY conjugates with plasmonic nanostructures.[12,41,42] The twisted and tilted intermolecular geometry found in the crystal structure of *O*-BDPhS1 qualitatively explains the enhancement due to a limited number of molecular geometries in the neat film. Further investigation of the side chain−optical response relationships can pave the way to maximizing the molecular dissymmetry factor. In the perspective of optoelectronic applications, it is crucial to perform such optimization while maintaining the isotropic nature of the film.

Experimental Methods. *Sample Preparation*

The glass substrates were initially thoroughly cleaned in an aqueous solution of Hellmanex in ultrapure water with sonication for 10 min, followed by sonication in ultrapure water for 10 min more and sonication in isopropanol for an additional 10 min. The glass substrates were rinsed in ultrapure water and dried. The toluene solution of *O*-BDPhR1/S1 (20 mg/mL) was dropped onto the substrate and spin-coated at 3000 rpm.

Theoretical Calculations.

TD-DFT calculations were conducted with the MN15 exchange−correlation functional as implemented in the Gaussian 16 software.[43] MN15 has been reported to show results in excellent agreement with experimental absorption and CD spectra.[39] The basis set used was 6-31G(d). Frequency analyses were also conducted to ensure that the converged structures reached the potential energy minimums. The CD intensities for the dimers (geometry 1 and 2) in Figure 3c were divided by two to compare with the monomer. Molecular structures were visualized using GaussView 6.1.1.[44]

Estimation of Dissymmetry Factors.

Following the methodology recently presented,[34] the apparent absorption dissymmetry factors ($g_{abs,exp}$) were calculated by:

$$\Delta Abs = \frac{CD(mdeg)}{32980} \quad (2)$$

$$g_{abs,exp} = \frac{\Delta Abs}{Abs_{mes}}, \quad (3)$$

which assumes the reflection becomes negligible ($A_{\mathrm{mes}} = -\log(T_{\mathrm{mes}})$) after baseline correction. To estimate the real absorption of the neat film, the reflection of the neat film was measured to correct the absorbance measurements taken (as standardly done) from the sole transmission measurements of *O*-BDPhR1/S1. The reflection correction for decadic absorbance was based on

$$A_{cor} = -\log(T_{mes} - R_{mes}). \quad (4)$$

This led us to estimate the corrected absorption dissymmetry factors ($g_{\mathrm{abs,cor}}$) by the following equation

$$g_{abs,cor} = \frac{\Delta Abs}{Abs_{cor}}. \quad (5)$$

The correction process gave a significant difference (~80%) in the neat film state (Figure 4b), while the hybrid films with less than 50 wt % loading of polystyrene did not. Note that the contribution of the reflection can also be estimated by thickness-dependent absorbance measurements, as reported previously.[35]

Mueller Polarimetry.

The Mueller matrix (MM) polarimetry enables the extraction of artifact-free polarimetric quantities such as circular dichroism (CD), from complex optical media.[34,35] To determine the MM, we used a dual-rotating quarter-wave plate (QWP) methodology, where a linear polarizer and a quarter-wave plate are used to set the polarization of the beam in a specific state characterized by a Stokes vector. A set of intensity measurements, associated with the different selection of

Stokes vectors in the preparation and analysis stages, allows the retrieval of the MM. For each measurement, we probed our sample with a specific Stokes vector and projected the outgoing beam into a known polarization state. The procedure is detailed in the Supporting Information. From the acquired experimental MM, one can eliminate the residual polarimetric contributions coming from the substrate and the bare optical setup. Using a differential decomposition method, we can then extract chiroptical observables with the capacity to isolate out any linear contribution that could arise from the given molecular system under study and that can become an artifact in the determination of CD strengths.

ASSOCIATED CONTENT

Supporting Information.

The Supporting Information is available free of charge at https://pubs.acs.org/doi/10.1021/acs.jpcc.3c04212.

Details of Mueller polarimetry, NMR spectra, AFM image, molecular structure, crystal packing, XRD, reflectivity, the setup of the Mueller matrix measurement, Mueller matrixes, chemical structures, absorption, and CD spectrum.

Accession Codes

CCDC 2237697 contains the supplementary crystallographic data for this paper. The data can be obtained free of charge via www.ccdc.cam.ac.uk/data_request/cif, by emailing data_request@ccdc.cam.ac.uk, or by contacting The Cambridge Crystallographic Data Centre, 12 Union Road, Cambridge CB2 1EZ, UK; fax: + 44 1223 336033.

AUTHOR INFORMATION

Present Addresses

§ Department of Applied Chemistry, Graduate School of Engineering, Center for Molecular Systems (CMS), Kyushu University, 744 Moto-oka, Nishi-ku, Fukuoka 819-0395, Japan.

Nanoscale Solar Cells, AMOLF, Science Park 104, 1098 XG Amsterdam, The Netherlands.

¶ Department of Physics University of Basel, Klingelbergstrasse 82, 4056 Basel, Switzerland.

Notes

The authors declare no competing financial interest.

ACKNOWLEDGMENT

We acknowledge support from the International Center for Frontier Research in Chemistry (icFRC, Strasbourg), the ANR Equipex Union (ANR-10-EQPX-52-01), the CSC (ANR-10-LABX-0026 CSC), and the JSPS Overseas Research Fellowships. This work is also part of the Interdisciplinary Thematic Institute QMat of the University of Strasbourg, CNRS, and Inserm. It was supported by the following programs: IdEx Unistra (ANR-10-IDEX-0002), the SFRI STRATUS project (ANR-20-SFRI-0012), and USIAS (ANR-10-IDEX-0002-02), under the framework of the French Investments for the Future Program. T.W.E. acknowledges the funding support of the ERC

(Project 788482 MOLUSC), QuantERA project RouTe, and the European Union's Horizon 2020 Research, Innovation Programme under the Marie Skłodowska-Curie Grant 811284 (UHMob). The authors thank F Richard, E. Devaux, C. Antheaume, and M. Morikawa for measuring the XRD and obtaining the AFM image and mass spectra. Y. S. thanks the Thomas Hermans laboratory for sharing equipment for syntheses at the University of Strasbourg, CNRS, UMR7140.

REFERENCES

(1)Carr, R.; Evans, N. H.; Parker, D. Lanthanide Complexes as Chiral Probes Exploiting Circularly Polarized Luminescence. *Chem. Soc. Rev.* **2012**, *41*, 7673–7686.

(2)Heffern, M. C.; Matosziuk, L. M.; Meade, T. J. Lanthanide Probes for Bioresponsive Imaging. *Chem. Rev.* **2014**, *114*, 4496–4539.

(3)Tiwari, M. P.; Prasad, A. Molecularly Imprinted Polymer Based Enantioselective Sensing Devices: A Review. *Anal. Chim. Acta* **2015**, *853*, 1–18.

(4)Brandt, J. R.; Salerno, F.; Fuchter, M. J. The Added Value of Small-Molecule Chirality in Technological Applications. *Nat. Rev. Chem.* **2017**, *1*, 1–12.

(5)Inoue, Y. Asymmetric Photochemical Reactions in Solution. *Chem. Rev.* **1992**, *92*, 741–770.

(6)Feringa, B. L.; van Delden, R. A. Absolute Asymmetric Synthesis: The Origin, Control, and Amplification of Chirality. *Angew. Chem. Int. Ed.* **1999**, *38*, 3418–3438.

(7)Schadt, M. Liquid Crystal Materials and Liquid Crystal Displays. *Annu. Rev. Mater. Sci.* **1997**, *27*, 305–379.

(8)Sherson, J. F.; Krauter, H.; Olsson, R. K.; Julsgaard, B.; Hammerer, K.; Cirac, I.; Polzik, E. S. Quantum Teleportation between Light and Matter. *Nature* **2006**, *443*, 557–560.

(9)Zhang, D.-W.; Li, M.; Chen, C.-F. Recent Advances in Circularly Polarized Electroluminescence Based on Organic Light-Emitting Diodes. *Chem. Soc. Rev.* **2020**, *49*, 1331–1343.

(10) Greenfield, J. L.; Wade, J.; Brandt, J. R.; Shi, X.; Penfold, T. J.; Fuchter, M. J. Pathways to Increase the Dissymmetry in the Interaction of Chiral Light and Chiral Molecules. *Chem. Sci.* **2021**, *12*, 8589–8602.

(11) Albano, G.; Pescitelli, G.; Di Bari, L. Chiroptical Properties in Thin Films of π-Conjugated Systems. *Chem. Rev.* **2020**, *120*, 10145–10243.

(12) Nizar, N. S.; Sujith, M.; Swathi, K.; Sissa, C.; Painelli, A.; Thomas, K. G. Emergent Chiroptical Properties in Supramolecular and Plasmonic Assemblies. *Chem. Soc. Rev.* **2021**, *50*, 11208–11226.

(13) Maeda, H.; Bando, Y.; Shimomura, K.; Yamada, I.; Naito, M.; Nobusawa, K.; Tsumatori, H.; Kawai, T. Chemical-Stimuli-Controllable Circularly Polarized Luminescence from Anion-Responsive π-Conjugated Molecules. *J. Am. Chem. Soc.* **2011**, *133*, 9266–9269.

(14) Sánchez-Carnerero, E. M.; Moreno, F.; Maroto, B. L.; Agarrabeitia, A. R.; Ortiz, M. J.; Vo, B. G.; Muller, G.; de la Moya, S. Circularly Polarized Luminescence by Visible-Light Absorption in a Chiral O-BODIPY Dye: Unprecedented Design of CPL Organic Molecules from Achiral Chromophores. *J. Am. Chem. Soc.* **2014**, *136*, 3346–3349.

(15) Zhang, L.; Zhao, L.; Wang, K.; Jiang, J. Chiral Benzo-Fused Aza-BODIPYs with Optical Activity Extending into the NIR Range. *Dyes Pigm.* **2016**, *134*, 427–433.

(16) Dhbaibi, K.; Favereau, L.; Srebro-Hooper, M.; Jean, M.; Vanthuyne, N.; Zinna, F.; Jamoussi, B.; Di Bari, L.; Autschbach, J.; Crassous, J. Exciton Coupling in Diketopyrrolopyrrole–

Helicene Derivatives Leads to Red and near-Infrared Circularly Polarized Luminescence. *Chem. Sci.* **2018**, *9*, 735–742.

(17) Liu, Z.; Jiang, Z.; He, C.; Chen, Y.; Guo, Z. Circularly Polarized Luminescence from Axially Chiral Binaphthalene-Bridged BODIPY. *Dyes Pigm.* **2020**, *181*, No. 108593.

(18) Gao, T.; Jiang, Z.; Chen, B.; Sun, Q.; Orooji, Y.; Huang, L.; Liu, Z. Axial Chiral Binaphthalene-Diketopyrrolopyrrole Dyads as Efficient Far-Red to near-Infrared Circularly Polarized Luminescent Emitters. *Dyes Pigm.* **2020**, *173*, No. 107998.

(19) Macé, A.; Hamrouni, K.; Gauthier, E. S.; Jean, M.; Vanthuyne, N.; Frédéric, L.; Pieters, G.; Caytan, E.; Roisnel, T.; Aloui, F.; et al. Circularly Polarized Fluorescent Helicene-Boranils: Synthesis, Photophysical and Chiroptical Properties. *Chem. Eur. J.* **2021**, *27*, 7959–7967.

(20) Zhang, S.; Wang, Y.; Meng, F.; Dai, C.; Cheng, Y.; Zhu, C. Circularly Polarized Luminescence of AIE-Active Chiral *O*-BODIPYs Induced via Intramolecular Energy Transfer. *Chem. Commun.* **2015**, *51*, 9014–9017.

(21) Wu, Y.; Wang, S.; Li, Z.; Shen, Z.; Lu, H. Chiral Binaphthyl-Linked BODIPY Analogues: Synthesis and Spectroscopic Properties. *J. Mater. Chem.* C **2016**, *4*, 4668–4674.

(22) Gartzia-Rivero, L.; Sánchez-Carnerero, E. M.; Jiménez, J.; Bañuelos, J.; Moreno, F.; Maroto, B. L.; López-Arbeloa, I.; de la Moya, S. Modulation of ICT Probability in Bi(Polyarene)-Based *O*-BODIPYs: Towards the Development of Low-Cost Bright Arene-BODIPY Dyads. *Dalton Trans.* **2017**, *46*, 11830–11839.

(23) Jiménez, J.; Moreno, F.; Maroto, B. L.; Cabreros, T. A.; Huy, A. S.; Muller, G.; Bañuelos, J.; de la Moya, S. Modulating ICT Emission: A New Strategy to Manipulate the CPL Sign in Chiral Emitters. *Chem. Commun.* **2019**, *55*, 1631–1634.

(24) Jiménez, J.; Díaz-Norambuena, C.; Serrano, S.; Ma, S. C.; Moreno, F.; Maroto, B. L.; Bañuelos, J.; Muller, G.; de la Moya, S. BINOLated Aminostyryl BODIPYs: A Workable Organic Molecular Platform for NIR Circularly Polarized Luminescence. *Chem. Commun.* **2021**, *57*, 5750–5753.

(25) Jiménez, J.; Avellanal-Zaballa, E.; Serrano, S.; Torres, A. R.; Agarrabeitia, A. R.; Moreno, F.; Muller, G.; Bañuelos, J.; Maroto, B. L.; de la Moya, S. Insight into the Influence of the Chiral Molecular Symmetry on the Chiroptics of Fluorescent BINOL-Based Boron Chelates. *Chem. Proc.* **2021**, *3*, No. 76.

(26) Berova, N.; Polavarapu, P. L.; Nakanishi, K.; Woody, R. W. *Comprehensive Chiroptical Spectroscopy, Vol. 1: Instrumentation, Methodologies, and Theoretical Simulations*; John Wiley & Sons, 2011.

(27) Zheng, D.; Zheng, L.; Yu, C.; Zhan, Y.; Wang, Y.; Jiang, H. Significant Enhancement of Circularly Polarized Luminescence Dissymmetry Factors in Quinoline Oligoamide Foldamers with Absolute Helicity. *Org. Lett.* **2019**, *21*, 2555–2559.

(28) Kar, S.; Swathi, K.; Sissa, C.; Painelli, A.; Thomas, K. G. Emergence of Chiroptical Properties in Molecular Assemblies of Phenyleneethynylenes: The Role of Quasi-Degenerate Excitations. *J. Phys. Chem. Lett.* **2018**, *9*, 4584–4590.

(29) Shindo, Y.; Nakagawa, M.; Ohmi, Y. On the Problems of CD Spectropolarimeters. II: Artifacts in CD Spectrometers. *Appl. Spectrosc.* **1985**, *39*, 860–868.

(30) Shindo, Y.; Kani, K.; Horinaka, J.; Kuroda, R.; Harada, T. The Application of Polarization Modulation Method to Investigate the Optical Homogeneity of Polymer Films. *J. Plast. Film Sheeting* **2001**, *17*, 164–183.

(31) Craig, M. R.; Jonkheijm, P.; Meskers, S. C. J.; Schenning, A. P. H. J.; Meijer, E. W. The Chiroptical Properties of a Thermally Annealed Film of Chiral Substituted Polyfluorene Depend on Film Thickness. *Adv. Mater.* **2003**, *15*, 1435–1438.

(32) Castiglioni, E.; Biscarini, P.; Abbate, S. Experimental Aspects of Solid State Circular Dichroism. *Chirality* **2009**, *21*, E28–E36.

(33) Shindo, Y.; Nishio, M. The Effect of Linear Anisotropies on the CD Spectrum: Is It True That the Oriented Polyvinyalcohol Film Has a Magic Chiral Domain Inducing Optical Activity in Achiral Molecules? *Biopolymers* **1990**, *30*, 25–31.

(34) Arteaga, O. Number of Independent Parameters in the Mueller Matrix Representation of Homogeneous Depolarizing Media. *Opt. Lett.* **2013**, *38*, 1131–1133.

(35) Schulz, M.; Zablocki, J.; Abdullaeva, O. S.; Brück, S.; Balzer, F.; Lützen, A.; Arteaga, O.; Schiek, M. Giant Intrinsic Circular Dichroism of Prolinol-Derived Squaraine Thin Films. *Nat. Commun.* **2018**, *9*, 2413.

(36) Thomas, A.; Chervy, T.; Azzini, S.; Li, M.; George, J.; Genet, C.; Ebbesen, T. W. Mueller Polarimetry of Chiral Supramolecular Assembly. *J. Phys. Chem. C* **2018**, *122*, 14205–14212.

(37) Salij, A.; Goldsmith, R. H.; Tempelaar, R. Theory of Apparent Circular Dichroism Reveals the Origin of Inverted and Noninverted Chiroptical Response under Sample Flipping. *J. Am. Chem. Soc.* **2021**, *143*, 21519–21531.

(38) Karolin, J.; Johansson, L. B.-A.; Strandberg, L.; Ny, T. Fluorescence and Absorption Spectroscopic Properties of Dipyrrometheneboron Difluoride (BODIPY) Derivatives in Liquids, Lipid Membranes, and Proteins. *J. Am. Chem. Soc.* **1994**, *116*, 7801–7806.

(39) Yang, Q.; Fusè, M.; Bloino, J. Theoretical Investigation of the Circularly Polarized Luminescence of a Chiral Boron Dipyrromethene (BODIPY) Dye. *Front. Chem.* **2020**, *8*, No. 801.

(40) Di Bari, L.; Pescitelli, G.; Salvadori, P. Conformational Study of 2,2‘-Homosubstituted 1,1‘-Binaphthyls by Means of UV and CD Spectroscopy. *J. Am. Chem. Soc.* **1999**, *121*, 7998–8004.

(41) Ayuso, D.; Neufeld, O.; Ordonez, A. F.; Decleva, P.; Lerner, G.; Cohen, O.; Ivanov, M.; Smirnova, O. Synthetic Chiral Light for Efficient Control of Chiral Light–Matter Interaction. *Nat. Photon.* **2019**, *13*, 866–871.

(42) Lininger, A.; Palermo, G.; Guglielmelli, A.; Nicoletta, G.; Goel, M.; Hinczewski, M.; Strangi, G. Chirality in Light–Matter Interaction. *Adv. Mater.* **2022**, No. 2107325.

(43) Frisch, M. J.; Trucks, G. W.; Schlegel, H. B.; Scuseria, G. E.; Robb, M. A.; Cheeseman, J. R.; Scalmani, G.; Barone, V.; Petersson, G. A.; Nakatsuji, H.; et al. *Gaussian 16*, rev. C.01; Gaussian, Inc., Wallingford, CT, 2019.

(44) Dennington, R.; Keith, T. A.; Millam, J. M. *GaussView,* ver. 6.1; Semichem Inc., Shawnee Mission, KS, 2016.

TOC Graphic

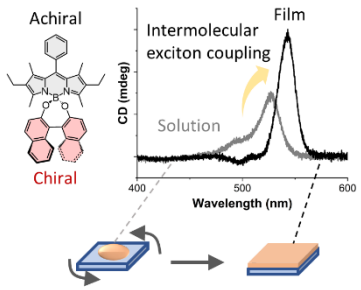
Achiral
Chiral
Intermolecular
exciton coupling
Film
Solution
CD (mdeg)
400
500
600
Wavelength (nm)